Design of Robust Differential Microphone Arrays

Liheng Zhao, Jacob Benesty, and Jingdong Chen, *Senior Member, IEEE*

***Abstract*—Differential microphone arrays (DMAs), due to their small size and enhanced directivity, are quite promising in speech enhancement applications. However, it is well known that differential beamformers have the drawback of white noise amplification, which is a major issue in the processing of wideband signals such as speech. In this paper, we focus on the design of robust DMAs. Based on the Maclaurin's series approximation and frequency-independent beampatterns, the robust first-, second-, and third-order DMAs are proposed by using more microphones than the order plus one, and the corresponding minimum-norm filters are derived. Compared to the traditional DMAs, the proposed designs are more robust with respect to white noise amplification while they are capable of achieving similar directional gains.**

***Index Terms*—Beamforming, beampattern, differential microphone arrays (DMAs), directivity factor, first-order DMA, robust DMAs, second-order DMA, third-order DMA, white noise gain.**

I. Introduction

IN REAL-WORLD environments, noise and reverberation are inevitable and they seriously degrade the quality and intelligibility of speech signals. Therefore, the ability of reducing noise and reverberation is highly desirable in many applications, such as hands-free telecommunication, hearing aids, and security.

Speech enhancement methods that are based on microphone arrays have been of important research interest for several decades [1]–[4]. Among the many beamforming techniques, differential beamforming has shown its great potential recently [5]–[7]. As early as in the 1940s, differential microphone arrays (DMAs) of different orders were constructed and their anti-noise characteristics were analyzed [8], [9]. Since then, a good amount of progress has been made. In [10], [11], adaptive DMAs were developed to suppress spatially non-stationary noise. In [12], an approach based on sensor calibration was designed to increase the DMAs' robustness against sensor mismatch, which may severely degrade their performance. In [13], DMAs were used to estimate the noise power spectral density (PSD), and the spectral subtraction algorithm was then applied to suppress noise. In [14], [15], approaches for the design of higher-order DMAs were developed. In [6], [7], DMAs were systematically studied from a signal processing perspective. Specifically, the design, implementation, and performance analysis of DMAs were presented.

Though a conventional Nth-order DMA, which consists of $N+1$ microphones, can achieve a high directional gain (i.e., a large SNR gain in diffuse noise), it has the problem of white noise amplification. In addition, this problem becomes much more serious as the order of the DMA increases [6]. To deal with this fundamental problem, we proposed recently to improve the conventional DMAs by using more microphones, M, than the order, N, i.e., $M > N+1$ [6]. This study is a continuation and an extension of our work presented in [6]. The major contribution of this paper is the derivation of minimum-norm filters based on Maclaurin's series approximation, which help increase the white noise gain. In comparison with the conventional DMAs, the proposed ones are more robust against white noise amplification while keeping the directional gain at a high level.

The paper is organized as follows. In Section II, the signal model, the formulation of the problem, and some useful definitions are presented. In Section III, the beampattern and its frequency-independent form are described. Based on Maclaurin's series approximation, the robust first-, second-, and third-order DMAs are developed in Sections IV, V, and VI, respectively. Simulations are carried out in Section VII, followed by some conclusions in Section VIII.

II. Signal Model, Problem Formulation, and Definitions

We consider a source signal (plane wave), in the farfield, that propagates in an anechoic acoustic environment at the speed of sound, i.e., $c = 340$ m/s, and impinges on a uniform linear sensor array consisting of M omnidirectional microphones, where the distance between two successive sensors is equal to δ (see Fig. 1). The direction of the source signal to the array is parameterized by the azimuthal angle θ. In this scenario, the steering vector (of length M) is given by

$$\mathbf{d}(\omega,\theta) = \left[1 \; e^{-\jmath\omega\tau_0\cos\theta} \; \cdots \; e^{-\jmath(M-1)\omega\tau_0\cos\theta}\right]^T, \quad (1)$$

where the superscript ^{T} is the transpose operator, $\jmath = \sqrt{-1}$ is the imaginary unit, $\omega = 2\pi f$ is the angular frequency, $f > 0$ is the temporal frequency, and $\tau_0 = \delta/c$ is the delay between two successive sensors at the angle $\theta = 0$. The acoustic wavelength is $\lambda = c/f$.

In order to avoid spatial aliasing [3], which has the negative effect of creating grating lobes (i.e., copies of the main lobe, which usually points toward the desired signal), it is necessary that the interelement spacing is less than $\lambda/2$, i.e.,

$$\omega\tau_0 < \pi. \quad (2)$$

Manuscript received February 20, 2014; revised June 22, 2014; accepted June 24, 2014. Date of publication July 10, 2014; date of current version July 18, 2014. The associate editor coordinating the review of this manuscript and approving it for publication was Prof. Thushara Dheemantha Abhayapala.

L. Zhao and J. Benesty are with INRS-EMT, University of Quebec, Montreal, QC H5A 1K6, Canada (e-mail: liheng.zhao@emt.inrs.ca; benesty@emt.inrs.ca).

J. Chen is with Northwestern Polytechnical University, Xi'an 710072, China (e-mail: jingdongchen@ieee.org).

Color versions of one or more of the figures in this paper are available online at http://ieeexplore.ieee.org.

Digital Object Identifier 10.1109/TASLP.2014.2337844

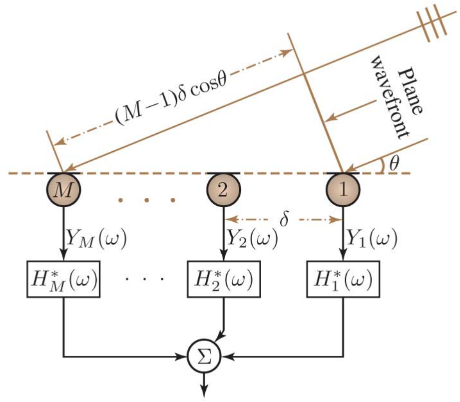

Fig. 1. A uniform linear microphone array with processing.

The condition (2) easily holds for small values of δ and at low frequencies but not at high frequencies.

We consider fixed directional beamformers, such as DMAs [6], [7], [12], [14], [15], where the main lobe is at the angle $\theta = 0$ (endfire direction) and the desired signal propagates from the same angle. Our focus is on the design of different orders DMAs that are robust to white noise amplification. For that, a complex weight, $H_m^*(\omega), m = 1, 2, \ldots, M$, is applied at the output of each microphone, where the superscript * denotes complex conjugation. The weighted outputs are then summed together to form the beamformer output as shown in Fig. 1. Putting all the gains together in a vector of length M, we get

$$\mathbf{h}(\omega) = [\, H_1(\omega) \quad H_2(\omega) \quad \cdots \quad H_M(\omega)\,]^T. \tag{3}$$

Then, the objective is to design such a filter so that the array obeys a given DMA pattern.

The mth microphone signal is given by

$$Y_m(\omega) = e^{-\jmath(m-1)\omega\tau_0} X(\omega) + V_m(\omega), m = 1, 2, \ldots, M, \tag{4}$$

where $X(\omega)$ is the desired signal and $V_m(\omega)$ is the additive noise at the mth microphone. It is assumed that the desired signal is uncorrelated with the additive noise. In a vector form, (4) is written as

$$\begin{aligned}\mathbf{y}(\omega) &= [\, Y_1(\omega) \quad Y_2(\omega) \quad \cdots \quad Y_M(\omega)\,]^T \\ &= \mathbf{d}(\omega, 0)X(\omega) + \mathbf{v}(\omega),\end{aligned} \tag{5}$$

where $\mathbf{d}(\omega, 0)$ is the steering vector at $\theta = 0$ (direction of the source) and the noise signal vector, $\mathbf{v}(\omega)$, is defined in a similar way to $\mathbf{y}(\omega)$.

The beamformer output is then [4]

$$\begin{aligned}Z(\omega) &= \sum_{m=1}^{M} H_m^*(\omega) Y_m(\omega) \\ &= \mathbf{h}^H(\omega)\mathbf{y}(\omega) \\ &= \mathbf{h}^H(\omega)\mathbf{d}(\omega, 0) X(\omega) + \mathbf{h}^H(\omega)\mathbf{v}(\omega),\end{aligned} \tag{6}$$

where $Z(\omega)$ is the estimate of the desired signal, $X(\omega)$, and the superscript ^{H} is the conjugate-transpose operator.

If we take microphone 1 as the reference, we can define the input SNR with respect to this reference as

$$\mathrm{iSNR}(\omega) = \frac{\phi_X(\omega)}{\phi_{V_1}(\omega)}, \tag{7}$$

where $\phi_X(\omega) = E[|X(\omega)|^2]$ and $\phi_{V_1}(\omega) = E[|V_1(\omega)|^2]$ are the variances of $X(\omega)$ and $V_1(\omega)$, respectively.

The output SNR is obtained from the variance of $Z(\omega)$:

$$\begin{aligned}\mathrm{oSNR}[\mathbf{h}(\omega)] &= \phi_X(\omega) \frac{\left|\mathbf{h}^H(\omega)\mathbf{d}(\omega, 0)\right|^2}{\mathbf{h}^H(\omega)\mathbf{\Phi}_{\mathbf{v}}(\omega)\mathbf{h}(\omega)} \\ &= \frac{\phi_X(\omega)}{\phi_{V_1}(\omega)} \times \frac{\left|\mathbf{h}^H(\omega)\mathbf{d}(\omega, 0)\right|^2}{\mathbf{h}^H(\omega)\mathbf{\Gamma}_{\mathbf{v}}(\omega)\mathbf{h}(\omega)},\end{aligned} \tag{8}$$

where $\mathbf{\Phi}_{\mathbf{v}}(\omega) = E[\mathbf{v}(\omega)\mathbf{v}^H(\omega)]$ and $\mathbf{\Gamma}_{\mathbf{v}}(\omega) = \frac{\mathbf{\Phi}_{\mathbf{v}}(\omega)}{\phi_{V_1}(\omega)}$ are the correlation and pseudo-coherence matrices of $\mathbf{v}(\omega)$, respectively.

The definition of the gain in SNR is easily derived from the previous definitions, i.e.,

$$\begin{aligned}\mathcal{G}[\mathbf{h}(\omega)] &= \frac{\mathrm{oSNR}[\mathbf{h}(\omega)]}{\mathrm{iSNR}(\omega)} \\ &= \frac{\left|\mathbf{h}^H(\omega)\mathbf{d}(\omega, 0)\right|^2}{\mathbf{h}^H(\omega)\mathbf{\Gamma}_{\mathbf{v}}(\omega)\mathbf{h}(\omega)}.\end{aligned} \tag{9}$$

We are interested in two types of noise.

- The temporally and spatially white noise with the same variance at all microphones[1]. In this case, $\mathbf{\Gamma}_{\mathbf{v}}(\omega) = \mathbf{I}_M$, where $\mathbf{I}_M$ is the $M \times M$ identity matrix. Therefore, the white noise gain (WNG) is

$$\mathcal{G}_{\mathrm{wn}}[\mathbf{h}(\omega)] = \frac{\left|\mathbf{h}^H(\omega)\mathbf{d}(\omega, 0)\right|^2}{\mathbf{h}^H(\omega)\mathbf{h}(\omega)}. \tag{10}$$

With the delay-and-sum (DS) beamformer, i.e.,

$$\mathbf{h}_{\mathrm{DS}}(\omega) = \frac{\mathbf{d}(\omega, 0)}{M}, \tag{11}$$

we find the maximum possible gain, which is

$$\mathcal{G}_{\mathrm{wn,max}}[\mathbf{h}(\omega)] = M. \tag{12}$$

We will see how the white noise may be amplified, especially at low frequencies, with differential beamformers.

- The diffuse noise[2], where

$$\begin{aligned}[\mathbf{\Gamma}_{\mathbf{v}}(\omega)]_{ij} = [\mathbf{\Gamma}_{\mathrm{dn}}(\omega)]_{ij} &= \frac{\sin[\omega(j-i)\tau_0]}{\omega(j-i)\tau_0} \\ &= \mathrm{sinc}[\omega(j-i)\tau_0].\end{aligned} \tag{13}$$

In this scenario, the gain in SNR, i.e.,

$$\mathcal{G}_{\mathrm{dn}}[\mathbf{h}(\omega)] = \frac{\left|\mathbf{h}^H(\omega)\mathbf{d}(\omega, 0)\right|^2}{\mathbf{h}^H(\omega)\mathbf{\Gamma}_{\mathrm{dn}}(\omega)\mathbf{h}(\omega)} \tag{14}$$

is called the directivity factor [3], [7]. It can be shown that the maximum possible gain is [16], [7]

$$\mathcal{G}_{\mathrm{dn,max}}[\mathbf{h}(\omega)] = M^2. \tag{15}$$

This gain can be achieved but at the expense of white noise amplification, especially at low frequencies.

These definitions of the SNRs and gains, which are extremely useful for the evaluation of any types of DMAs, conclude this section.

[1]This noise models the sensor noise.

[2]This situation corresponds to the spherically isotropic noise field.

III. Beampatterns

Each beamformer has a pattern of directional sensitivity, i.e., it has different sensitivities from sounds arriving from different directions. The beampattern or directivity pattern describes the sensitivity of the beamformer to a plane wave (source signal) impinging on the array from the direction θ. For a uniform linear array, it is mathematically defined as

$$\begin{aligned}\mathcal{B}_M\left[\mathbf{h}(\omega),\theta\right] &= \mathbf{d}^H\left(\omega,\theta\right)\mathbf{h}(\omega)\\ &= \sum_{m=1}^{M} H_m(\omega) e^{\jmath(m-1)\omega\tau_0\cos\theta}.\end{aligned} \quad (16)$$

The frequency-independent beampattern of an Nth-order DMA is well known. It is given by [6], [7]

$$\mathcal{B}_{\mathrm{D},N}(\theta) = \sum_{n=0}^{N} a_n \cos^n\theta, \quad (17)$$

where $a_n, n = 0, 1, \ldots, N$, are real coefficients. The different values of these coefficients determine the different directivity patterns of the Nth-order DMA. We deduce from (17) that the first-, second-, and third-order DMAs are, respectively,

$$\mathcal{B}_{\mathrm{D},1}(\theta) = a_0 + a_1\cos\theta, \quad (18)$$

$$\mathcal{B}_{\mathrm{D},2}(\theta) = a_0 + a_1\cos\theta + a_2\cos^2\theta, \quad (19)$$

$$\mathcal{B}_{\mathrm{D},3}(\theta) = a_0 + a_1\cos\theta + a_2\cos^2\theta + a_3\cos^3\theta. \quad (20)$$

The relation between (16) and (17) is shown in the following. It is well known that the Maclaurin's series for the exponential function is

$$e^x = \sum_{n=0}^{\infty}\frac{1}{n!}x^n. \quad (21)$$

Substituting $x = \jmath(m-1)\omega\tau_0\cos\theta$ into (21), we find that

$$e^{\jmath(m-1)\omega\tau_0\cos\theta} = \sum_{n=0}^{\infty}\frac{1}{n!}\left[\jmath(m-1)\omega\tau_0\cos\theta\right]^n. \quad (22)$$

Using (22) in the general definition of the beampattern, we obtain [6]

$$\begin{aligned}&\mathcal{B}_M\left[\mathbf{h}(\omega),\theta\right]\\ &= \sum_{m=1}^{M} H_m(\omega)e^{\jmath(m-1)\omega\tau_0\cos\theta}\\ &= \sum_{m=1}^{M} H_m(\omega)\sum_{n=0}^{\infty}\frac{1}{n!}\left[\jmath(m-1)\omega\tau_0\cos\theta\right]^n\\ &= \sum_{n=0}^{\infty}\cos^n\theta\left[\frac{(\jmath\omega\tau_0)^n}{n!}\sum_{m=1}^{M}(m-1)^n H_m(\omega)\right].\end{aligned} \quad (23)$$

If we limit the series to the order N, $\mathcal{B}_M[\mathbf{h}(\omega),\theta]$ can be approximated by

$$\begin{aligned}&\mathcal{B}_{M,N}\left[\mathbf{h}(\omega),\theta\right]\\ &= \sum_{n=0}^{N}\cos^n\theta\left[\frac{(\jmath\omega\tau_0)^n}{n!}\sum_{m=1}^{M}(m-1)^n H_m(\omega)\right].\end{aligned} \quad (24)$$

We will see how to use the previous expression in order to design robust DMAs of different orders.

IV. Robust First-Order DMAs

Let us assume that δ is very small (implying that τ_0 is also very small), so that $\mathcal{B}_{M,N}[\mathbf{h}(\omega),\theta]$ with $N = 1$ approximates $\mathcal{B}_M[\mathbf{h}(\omega),\theta]$ well. Then, we have

$$\mathcal{B}_{M,1}\left[\mathbf{h}(\omega),\theta\right] = \sum_{m=1}^{M} H_m(\omega)\left[1 + \jmath(m-1)\omega\tau_0\cos\theta\right]. \quad (25)$$

We study two cases: $M = 2$ and $M > 2$. The former is the traditional approach while the latter is considered as the robust version.

For $M = 2$, we can express (25) as

$$\mathcal{B}_{2,1}\left[\mathbf{h}(\omega),\theta\right] = H_1(\omega) + H_2(\omega) + \jmath H_2(\omega)\omega\tau_0\cos\theta. \quad (26)$$

Now, we wish to find $H_1(\omega)$ and $H_2(\omega)$ in such a way that $\mathcal{B}_{2,1}[\mathbf{h}(\omega),\theta]$ is a frequency-invariant first-order DMA pattern, i.e.,

$$\mathcal{B}_{2,1}\left[\mathbf{h}(\omega),\theta\right] = a_0 + a_1\cos\theta = \mathcal{B}_{\mathrm{D},1}(\theta). \quad (27)$$

Comparing the previous expression with (26), we find that

$$H_2(\omega) = \frac{a_1}{\jmath\omega\tau_0} \quad (28)$$

and

$$H_1(\omega) = -H_2(\omega) + a_0. \quad (29)$$

Therefore, with this approach, we can design any first-order DMA.

The case $M > 2$ is more interesting. We still want to find the coefficients $H_m(\omega), m = 1, 2, \ldots, M$ in such a way that $\mathcal{B}_{M,1}[\mathbf{h}(\omega),\theta] = \mathcal{B}_{\mathrm{D},1}(\theta)$. It can be checked that

$$\begin{bmatrix} 1 & 2 & \cdots & M-1 \end{bmatrix}\begin{bmatrix} H_2(\omega)\\ H_3(\omega)\\ \vdots\\ H_M(\omega)\end{bmatrix} = \frac{a_1}{\jmath\omega\tau_0} \quad (30)$$

and

$$\sum_{m=1}^{M} H_m(\omega) = a_0. \quad (31)$$

Taking the minimum-norm solution of (30), it is clear that the filter coefficients are as follows:

$$H_i(\omega) = \frac{6(i-1)a_1}{M(M-1)(2M-1)\jmath\omega\tau_0}, i = 2, 3, \ldots, M \quad (32)$$

and

$$H_1(\omega) = -\sum_{i=2}^{M} H_i(\omega) + a_0 = -\frac{3a_1}{(2M-1)\jmath\omega\tau_0} + a_0. \quad (33)$$

It is easily seen that (28) and (29) can be derived from (32) and (33), respectively, by setting $M = 2$.

In Appendix, we show that, with the proposed filter, the white noise gain is an increasing function of M.

V. Robust Second-Order DMAs

We follow the same methodology as in the previous section but, this time, we assume that $\mathcal{B}_{M,N}[\mathbf{h}(\omega),\theta]$ with $N = 2$ approximates $\mathcal{B}_M[\mathbf{h}(\omega),\theta]$ well. Therefore,

$$\mathcal{B}_{M,2}[\mathbf{h}(\omega),\theta] = \sum_{m=1}^{M} H_m(\omega)\left[1+\jmath(m-1)\omega\tau_0\cos\theta - \frac{(m-1)^2(\omega\tau_0)^2}{2}\cos^2\theta\right]. \quad (34)$$

We are ready to study the traditional ($M = 3$) and robust ($M > 3$) cases.

For $M = 3$, we can rewrite (34) as

$$\begin{aligned}\mathcal{B}_{3,2}[\mathbf{h}(\omega),\theta] = &H_1(\omega)+H_2(\omega)+H_3(\omega) \\ &+ \jmath H_2(\omega)\omega\tau_0\cos\theta + 2\jmath H_3(\omega)\omega\tau_0\cos\theta \\ &- H_2(\omega)\frac{(\omega\tau_0)^2}{2}\cos^2\theta - H_3(\omega)\frac{4(\omega\tau_0)^2}{2}\cos^2\theta.\end{aligned} \quad (35)$$

Our aim is to find $H_1(\omega)$, $H_2(\omega)$, and $H_3(\omega)$ in such a way that $\mathcal{B}_{3,2}[\mathbf{h}(\omega),\theta]$ is a frequency-invariant second-order DMA pattern, i.e.,

$$\mathcal{B}_{3,2}[\mathbf{h}(\omega),\theta] = a_0 + a_1\cos\theta + a_2\cos^2\theta = \mathcal{B}_{\mathrm{D},2}(\theta). \quad (36)$$

By simple identification, we find that

$$\begin{bmatrix} 1 & 2 \\ 1 & 4 \end{bmatrix}\begin{bmatrix} H_2(\omega) \\ H_3(\omega) \end{bmatrix} = \begin{bmatrix} \frac{a_1}{\jmath\omega\tau_0} \\ \frac{-2a_2}{(\omega\tau_0)^2} \end{bmatrix} \quad (37)$$

and

$$H_1(\omega) + H_2(\omega) + H_3(\omega) = a_0. \quad (38)$$

As a consequence, the solution is

$$\begin{bmatrix} H_2(\omega) \\ H_3(\omega) \end{bmatrix} = \frac{1}{2}\begin{bmatrix} 4 & -2 \\ -1 & 1 \end{bmatrix}\begin{bmatrix} \frac{a_1}{\jmath\omega\tau_0} \\ \frac{-2a_2}{(\omega\tau_0)^2} \end{bmatrix} \quad (39)$$

and

$$H_1(\omega) = -H_2(\omega) - H_3(\omega) + a_0. \quad (40)$$

We see that we can design any second-order DMA.

For $M > 3$, we still want to find the coefficients $H_m(\omega), m = 1, 2, \ldots, M$ in such a way that $\mathcal{B}_{M,2}[\mathbf{h}(\omega),\theta] = \mathcal{B}_{\mathrm{D},2}(\theta)$. Following the same principle as in the previous section, one can find the minimum-norm solution as

$$\begin{bmatrix} H_2(\omega) \\ H_3(\omega) \\ \vdots \\ H_M(\omega) \end{bmatrix} = \Upsilon_2^T\left(\Upsilon_2\Upsilon_2^T\right)^{-1}\begin{bmatrix} \frac{a_1}{\jmath\omega\tau_0} \\ \frac{-2a_2}{(\omega\tau_0)^2} \end{bmatrix} \quad (41)$$

and

$$H_1(\omega) = -\sum_{i=2}^{M} H_i(\omega) + a_0, \quad (42)$$

where

$$\Upsilon_2 = \begin{bmatrix} 1 & 2 & \cdots & M-1 \\ 1 & 2^2 & \cdots & (M-1)^2 \end{bmatrix} \quad (43)$$

is a $2 \times (M-1)$ matrix.

It can be checked that (39) and (40) are, respectively, special cases of (41) and (42) by setting $M = 3$.

In Appendix, we show that, with the proposed robust approach, we can dramatically increase the white noise gain.

VI. Robust Third-Order DMAs

Following the same ideas as before, it is easy to see that the coefficients of the filter for the design of robust third-order DMAs are given by

$$\begin{bmatrix} H_2(\omega) \\ H_3(\omega) \\ \vdots \\ H_M(\omega) \end{bmatrix} = \Upsilon_3^T\left(\Upsilon_3\Upsilon_3^T\right)^{-1}\begin{bmatrix} \frac{a_1}{\jmath\omega\tau_0} \\ \frac{-2a_2}{(\omega\tau_0)^2} \\ \frac{-6a_3}{\jmath(\omega\tau_0)^3} \end{bmatrix} \quad (44)$$

and

$$H_1(\omega) = -\sum_{i=2}^{M} H_i(\omega) + a_0, \quad (45)$$

where

$$\Upsilon_3 = \begin{bmatrix} 1 & 2 & \cdots & M-1 \\ 1 & 2^2 & \cdots & (M-1)^2 \\ 1 & 2^3 & \cdots & (M-1)^3 \end{bmatrix} \quad (46)$$

is a $3 \times (M-1)$ matrix. Now, the number of microphones must be at least equal to four.

VII. Simulations

In this section, we carry out some simulations to evaluate the performance of the robust first-, second-, and third-order DMAs. For comparison, we also give the performance of the corresponding conventional DMAs, i.e., $M = N + 1$. We set the interelement spacing to $\delta = 0.5$ cm and the incident angle of the desired signal to $\theta = 0$. In addition, we use the supercardioid patterns of different orders to derive the filters. The

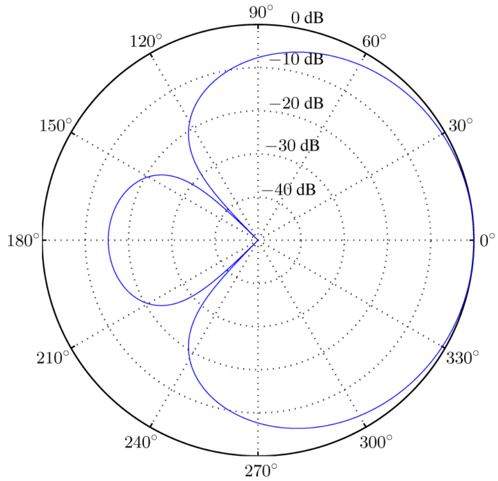

Fig. 2. Pattern of the first-order supercardioid.

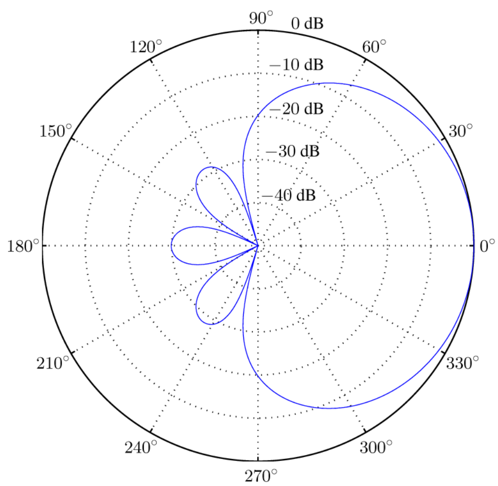

Fig. 3. Pattern of the second-order supercardioid.

frequency-independent first-, second-, and third-order supercardioid patterns are given by [15]

$$\mathcal{B}_{\mathrm{D},1}(\theta) = 0.414 + 0.586\cos\theta, \tag{47}$$

$$\mathcal{B}_{\mathrm{D},2}(\theta) = 0.103 + 0.484\cos\theta + 0.413\cos^2\theta, \tag{48}$$

$$\mathcal{B}_{\mathrm{D},3}(\theta) = 0.022 + 0.217\cos\theta + 0.475\cos^2\theta + 0.286\cos^3\theta. \tag{49}$$

These supercardioid patterns are illustrated in Figs. 2–4.

A. First-Order DMAs

In the first set of simulations, we study the performance of the first-order DMA for different values of M. In Figs. 5 and 6, we show the results for $M = 2$, which is actually the conventional approach. The beampattern in Fig. 5, which is symmetrical with respect to the axis $0° - 180°$, shows that the signal from the desired direction (i.e., $\theta = 0$) is perfectly preserved while the signals from the other directions are attenuated and, particularly, the largest amount of signal attenuations are achieved at the directions $135°$ and $225°$ as we have two nulls at these two directions. Comparing the patterns of Figs. 5 and 2, we observe that the designed pattern has less explicit nulls than the supercardioid. This is due to the MacLaurin's series approximation.

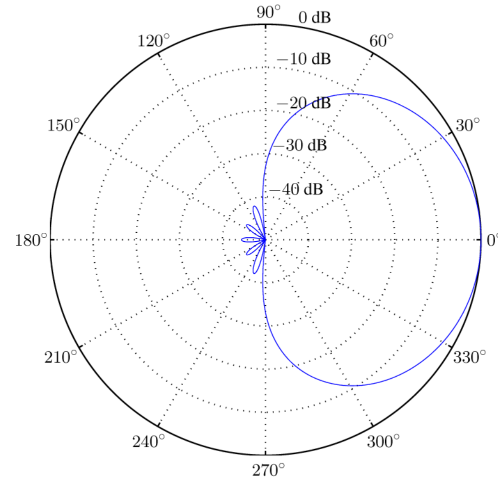

Fig. 4. Pattern of the third-order supercardioid.

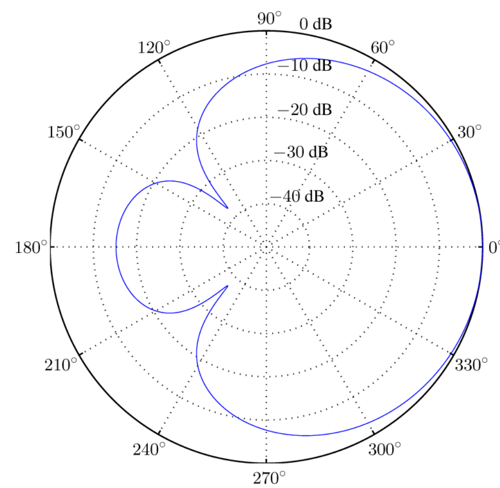

Fig. 5. Beampattern of the first-order DMA. $M = 2$, $\delta = 0.5$ cm, and $f = 1$ kHz.

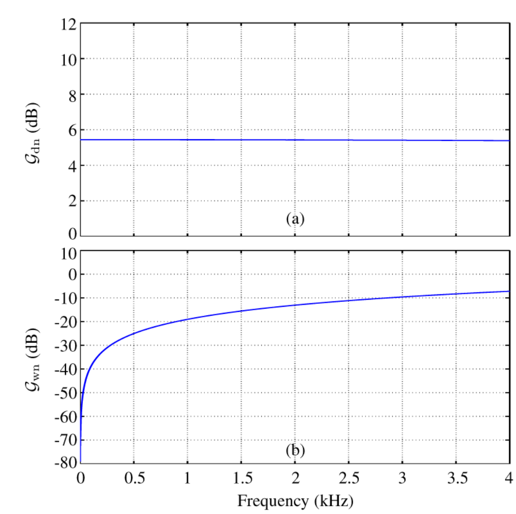

Fig. 6. SNR gains of the first-order DMA as a function of frequency: (a) directivity factor and (b) white noise gain. $M = 2$ and $\delta = 0.5$ cm.

From Fig. 6, we can see that the first-order DMA gives a constant directivity factor of approximately 5 dB while the white noise gain is negative. It can be noticed that white noise amplification is especially high at low frequencies. Then, we investigate the performance of the robust first-order DMA with 4 and

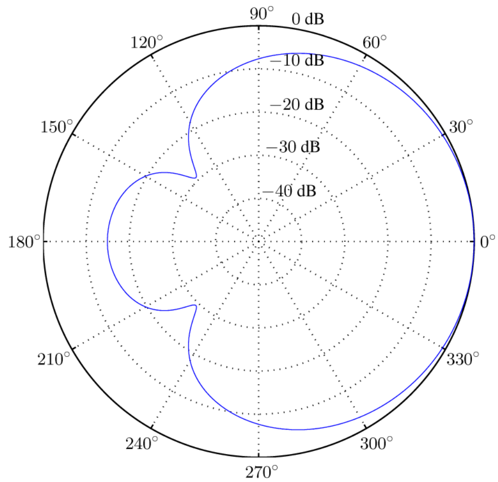

Fig. 7. Beampattern of the robust first-order DMA. $M = 4$, $\delta = 0.5$ cm, and $f = 1$ kHz.

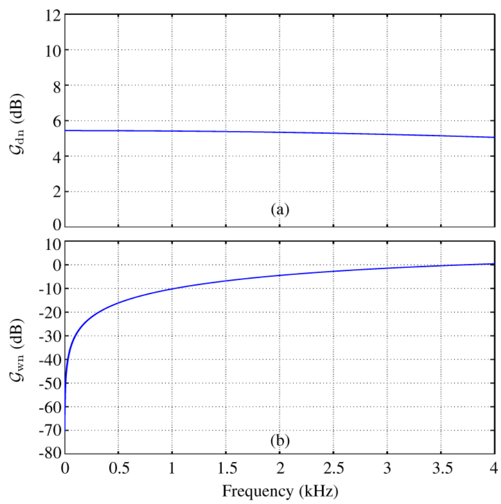

Fig. 8. SNR gains of the robust first-order DMA as a function of frequency: (a) directivity factor and (b) white noise gain. $M = 4$ and $\delta = 0.5$ cm.

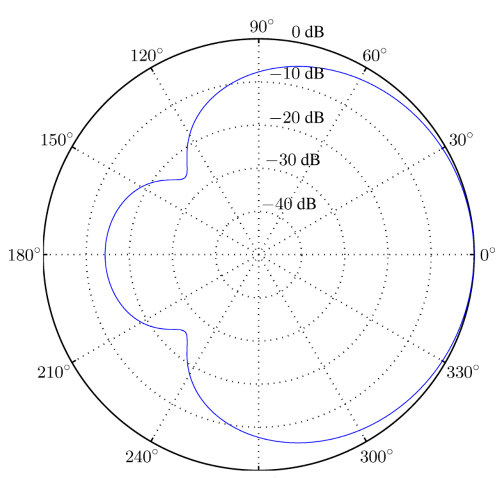

Fig. 9. Beampattern of the robust first-order DMA. $M = 6$, $\delta = 0.5$ cm, and $f = 1$ kHz.

6 microphones. Figs. 7–10 present the results. We can see that the white noise gain is considerably improved as M increases, while the beampattern and the directivity factor do not change much. Taking $f = 1$ kHz as an example, we summarize the directivity factor and white noise gain of the first-order DMAs in Table I. It is clearly seen that increasing the number of microphones improves the white noise gain significantly while the directivity factor does not change much. So, the larger is the number of microphones, the more robust is the first-order DMA against white noise amplification.

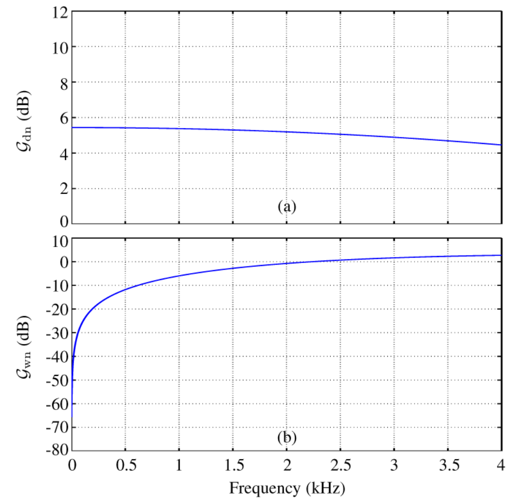

Fig. 10. SNR gains of the robust first-order DMA as a function of frequency: (a) directivity factor and (b) white noise gain. $M = 6$ and $\delta = 0.5$ cm.

TABLE I
DIRECTIVITY FACTOR (DF) AND WHITE NOISE GAIN (WNG) OF THE FIRST-ORDER DMA WITH DIFFERENT NUMBERS OF MICROPHONES. $\delta = 0.5$ cm AND $f = 1$ kHz

	$M = 2$	$M = 4$	$M = 6$
DF (dB)	5.43	5.41	5.38
WNG (dB)	−19.06	−10.21	−5.98

B. Second-Order DMAs

This set of simulations is designed to investigate the effect of M on the performance of the second-order DMA. We first set $M = 3$ to study the performance of the conventional second-order DMA. The beampattern and SNR gains are plotted in Figs. 11 and 12, respectively. It is clearly seen that the conventional second-order DMA maintains the signal from the desired direction (i.e., $\theta = 0$) without distortion while suppressing the signals from the other directions. Moreover, the conventional second-order DMA yields more than 8 dB SNR gain in diffuse noise, but it has the problem of white noise amplification, which is much worse than the conventional first-order DMA. Then, we take 5 and 8 microphones to form the robust second-order DMAs. Figs. 13–16 plot the results. We can see that, by increasing the value of M, we get significant improvement in the white noise gain while the beampattern and the directivity factor are not much affected.

C. Third-Order DMAs

In the third set of simulations, we study the performance of the third-order DMA by setting $M = 4$, $M = 7$, and $M = 10$, respectively. The beampattern and the SNR gains are plotted in Figs. 17–22. One can see that the value of M affects the performance of the third-order DMA in a similar way as it does

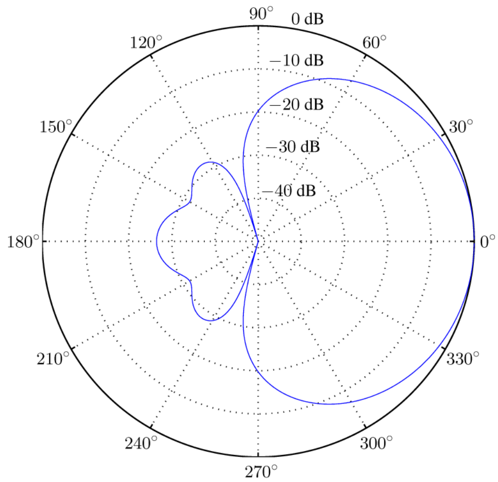

Fig. 11. Beampattern of the second-order DMA. $M = 3$, $\delta = 0.5$ cm, and $f = 1$ kHz.

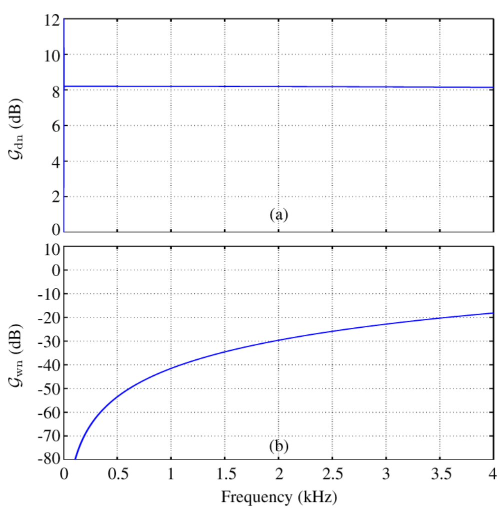

Fig. 12. SNR gains of the second-order DMA as a function of frequency: (a) directivity factor and (b) white noise gain. $M = 3$ and $\delta = 0.5$ cm.

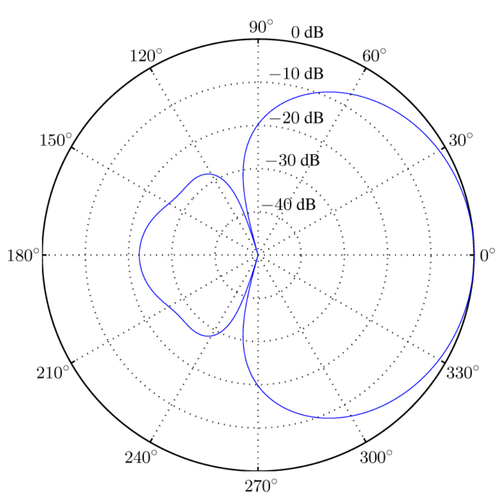

Fig. 13. Beampattern of the robust second-order DMA. $M = 5$, $\delta = 0.5$ cm, and $f = 1$ kHz.

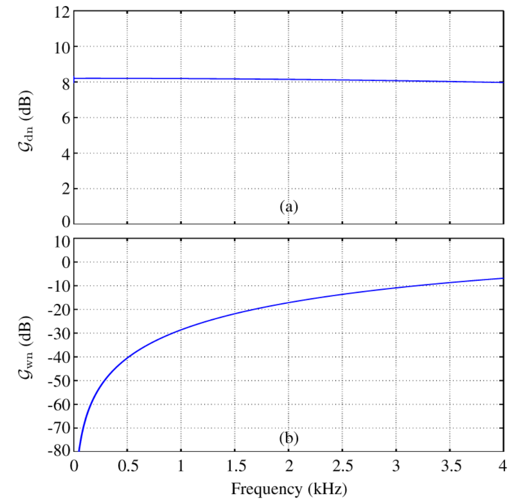

Fig. 14. SNR gains of the robust second-order DMA as a function of frequency: (a) directivity factor and (b) white noise gain. $M = 5$ and $\delta = 0.5$ cm.

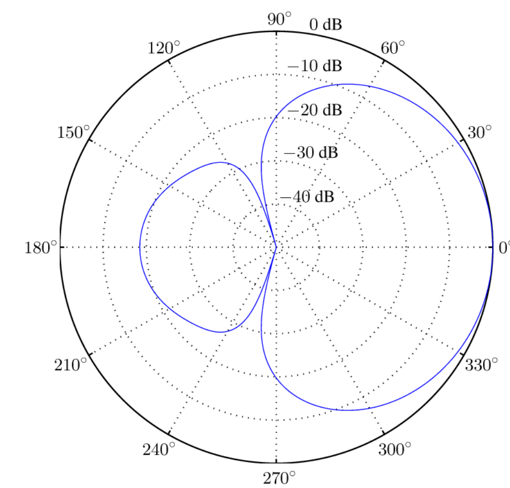

Fig. 15. Beampattern of the robust second-order DMA. $M = 8$, $\delta = 0.5$ cm, and $f = 1$ kHz.

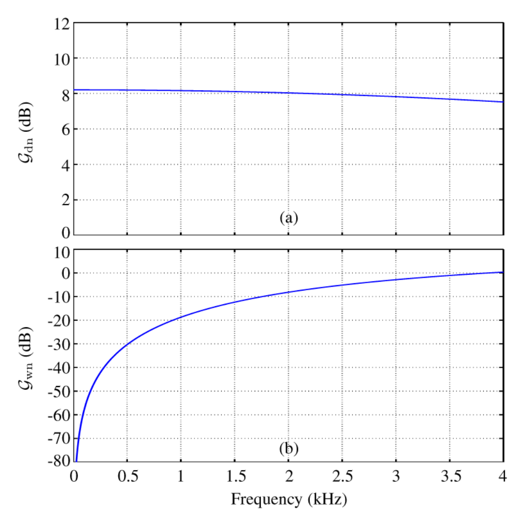

Fig. 16. SNR gains of the robust second-order DMA as a function of frequency: (a) directivity factor and (b) white noise gain. $M = 8$ and $\delta = 0.5$ cm.

for the first- and second-order DMAs, i.e., the white noise gain is significantly improved as the value of M increases while the beampattern and the directivity factor are not affected much by the number of microphones. We can also notice, particularly in Fig. 18, that the directivity factor of the third-order DMA fluctuates a lot at very low frequencies (e.g., less than 100 Hz). This, however, can be fixed by slightly regularizing the matrix

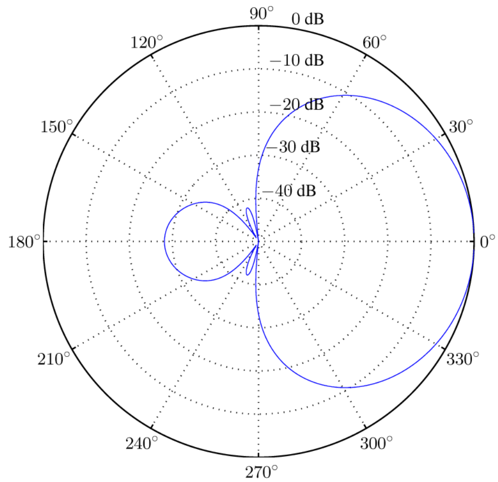

Fig. 17. Beampattern of the third-order DMA. $M = 4$, $\delta = 0.5$ cm, and $f = 1$ kHz.

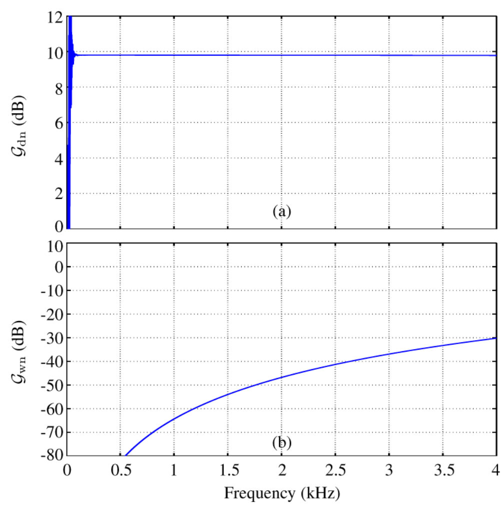

Fig. 18. SNR gains of the third-order DMA as a function of frequency: (a) directivity factor and (b) white noise gain. $M = 4$ and $\delta = 0.5$ cm.

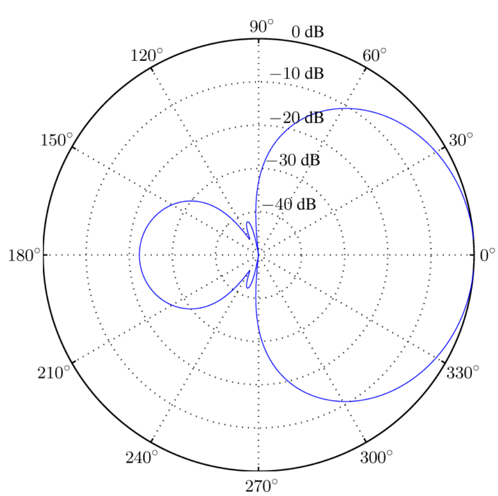

Fig. 19. Beampattern of the robust third-order DMA. $M = 7$, $\delta = 0.5$ cm, and $f = 1$ kHz.

to be inverted. In conclusion, by increasing the number of microphones as compared to the order, we can make DMAs much more robust to white noise amplification.

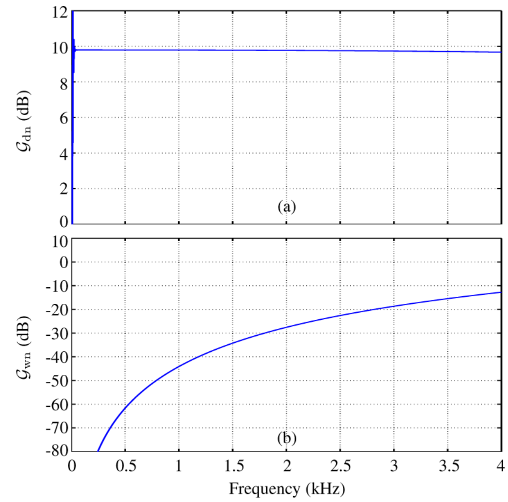

Fig. 20. SNR gains of the robust third-order DMA as a function of frequency: (a) directivity factor and (b) white noise gain. $M = 7$ and $\delta = 0.5$ cm.

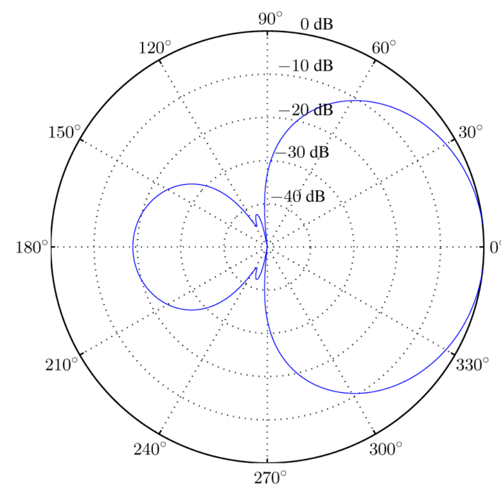

Fig. 21. Beampattern of the robust third-order DMA. $M = 10$, $\delta = 0.5$ cm, and $f = 1$ kHz.

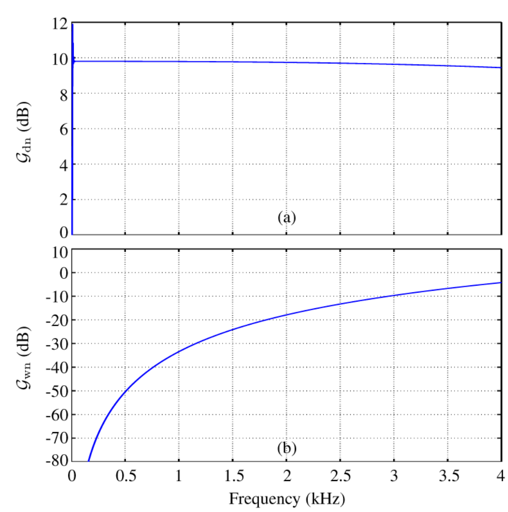

Fig. 22. SNR gains of the robust third-order DMA as a function of frequency: (a) directivity factor and (b) white noise gain. $M = 10$ and $\delta = 0.5$ cm.

D. Another Relevant Example

In this subsection, we give simulations for another relevant example in order to validate the generality of the proposed ap-

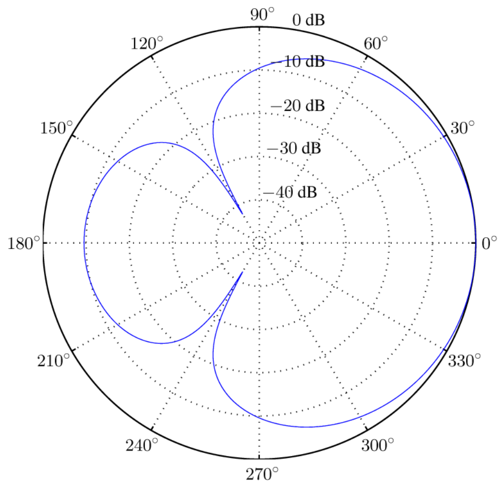

Fig. 23. Beampattern of the first-order DMA (hypercardioid). $M = 2$, $\delta = 0.5$ cm, and $f = 1$ kHz.

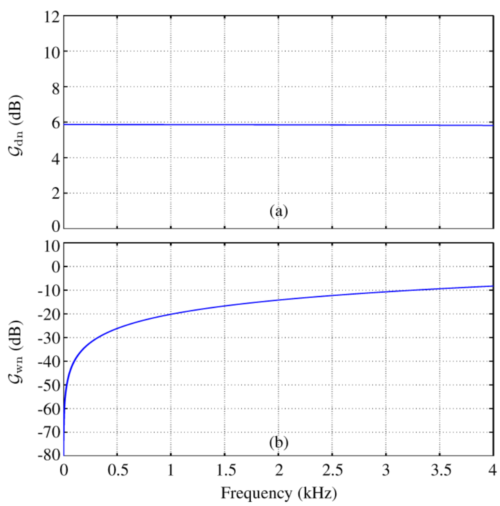

Fig. 24. SNR gains of the first-order DMA (hypercardioid) as a function of frequency: (a) directivity factor and (b) white noise gain. $M = 2$ and $\delta = 0.5$ cm.

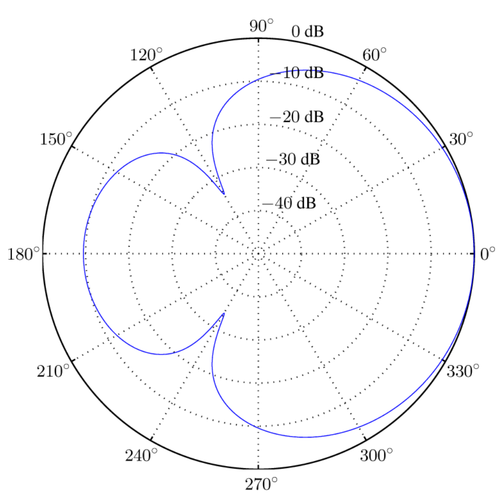

Fig. 25. Beampattern of the robust first-order DMA (hypercardioid). $M = 4$, $\delta = 0.5$ cm, and $f = 1$ kHz.

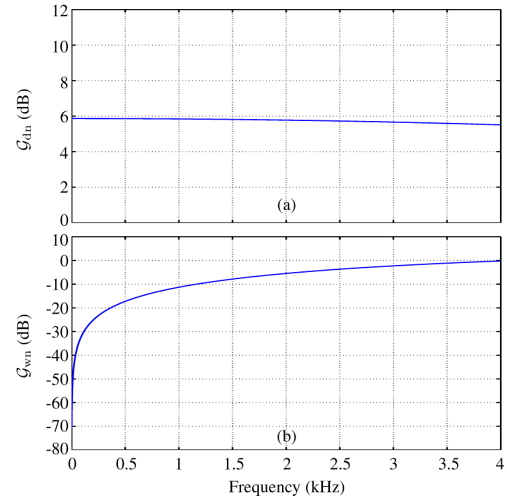

Fig. 26. SNR gains of the robust first-order DMA (hypercardioid) as a function of frequency: (a) directivity factor and (b) white noise gain. $M = 4$ and $\delta = 0.5$ cm.

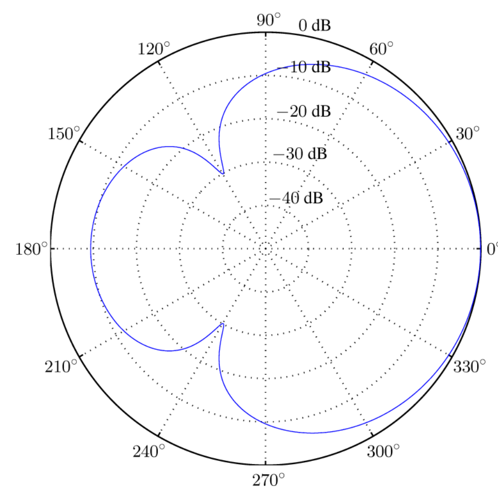

Fig. 27. Beampattern of the robust first-order DMA (hypercardioid). $M = 6$, $\delta = 0.5$ cm, and $f = 1$ kHz.

proach. This time, we use the first-order hypercardioid pattern[3] to derive DMAs and plot the results in Figs. 23–28. Similarly, we observe that, with increased number of microphones, the proposed first-order DMA improves the white noise gain significantly while the beampattern and directivity factor stay almost the same. Similar results can be obtained for other orders or patterns, which will be left to the reader's investigation.

VIII. Conclusions

In this paper, we focused on the design of robust DMAs based on the Maclaurin's series approximation. By increasing the number of microphones in the first-, second-, and third-order DMAs, we derived the corresponding minimum-norm filters, which have the potential to combat the problem of white noise amplification. Simulation results showed that the minimum-norm approach can achieve similar directivity factors as compared to the traditional method while its robustness against white noise amplification is much better.

[3]The first-order hypercardioid pattern has the form of $\mathcal{B}_{\rm D,1}(\theta) = 0.333 + 0.667\cos\theta$.

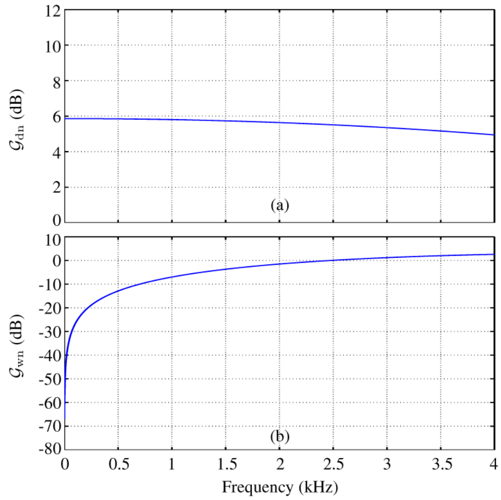

Fig. 28. SNR gains of the robust first-order DMA (hypercardioid) as a function of frequency: (a) directivity factor and (b) white noise gain. $M = 6$ and $\delta = 0.5$ cm.

Appendix A

In this section, we prove that the white noise gain of the robust Nth-order DMA is an increasing function of the number of microphones. But, before presenting the proofs, we give some useful formulae:

$$\sum_{m=1}^{M-1} m^2 = \frac{1}{6} M (M-1)(2M-1), \quad (50)$$

$$\sum_{m=1}^{M-1} m^3 = \frac{1}{4} M^2 (M-1)^2, \quad (51)$$

$$\sum_{m=1}^{M-1} m^4 = \frac{1}{30} M (M-1) \left(6M^3 - 9M^2 + M + 1\right), \quad (52)$$

where $M \geq 2$.

We recall that the white noise gain of the robust Nth-order DMA has the form:

$$\mathcal{G}_{\rm wn}\left[\mathbf{h}(\omega)\right] = \frac{\left|\mathbf{h}^H(\omega)\mathbf{d}(\omega, 0)\right|^2}{\mathbf{h}^H(\omega)\mathbf{h}(\omega)} = \frac{\left|\mathcal{B}_{M,N}\left[\mathbf{h}(\omega), 0\right]\right|^2}{\mathbf{h}^H(\omega)\mathbf{h}(\omega)}, \quad (53)$$

where $\mathcal{B}_{M,N}[\mathbf{h}(\omega), 0]$ is the beampattern of the robust Nth-order DMA at $\theta = 0$, and it is an approximation of $\mathcal{B}_M[\mathbf{h}(\omega), 0]$. Since the beampattern of the Nth-order DMA is frequency independent, i.e.,

$$\mathcal{B}_{M,N}[\mathbf{h}(\omega), \theta] = \mathcal{B}_{D,N}(\theta) = \sum_{n=0}^{N} a_n \cos^n \theta, \quad (54)$$

we have

$$\mathcal{B}_{M,N}\left[\mathbf{h}(\omega), 0\right] = \sum_{n=0}^{N} a_n. \quad (55)$$

Substituting (55) into (53), we can rewrite the white noise gain as

$$\mathcal{G}_{\rm wn}\left[\mathbf{h}(\omega)\right] = \frac{\left|\sum_{n=0}^{N} a_n\right|^2}{\mathbf{h}^H(\omega)\mathbf{h}(\omega)}. \quad (56)$$

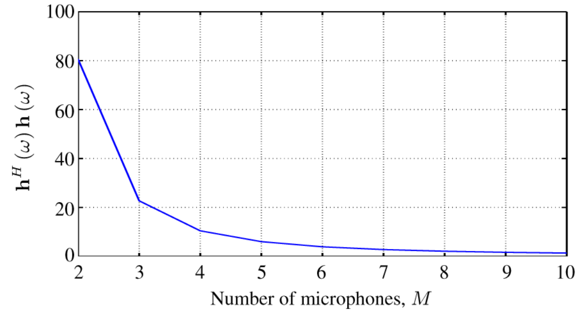

Fig. 29. The denominator of the white noise gain with the first-order DMA (supercardioid). $\delta = 0.5$ cm and $f = 1$ kHz.

First, we consider the first-order DMA, i.e., $N = 1$. Using (32) and (33), we can express the denominator of the white noise gain as

$$\begin{aligned} \mathbf{h}^H(\omega)\mathbf{h}(\omega) &= \sum_{m=1}^{M} \left|H_m(\omega)\right|^2 \\ &= a_0^2 + \frac{9a_1^2}{(2M-1)^2(\omega\tau_0)^2} + \sum_{i=2}^{M} \frac{36(i-1)^2 a_1^2}{M^2(M-1)^2(2M-1)^2(\omega\tau_0)^2} \\ &= a_0^2 + \frac{9a_1^2}{(2M-1)^2(\omega\tau_0)^2} + \frac{6a_1^2}{M(M-1)(2M-1)(\omega\tau_0)^2} \\ &= a_0^2 + \frac{a_1^2}{(\omega\tau_0)^2} \times \frac{3(3M-2)(M+1)}{M(M-1)(2M-1)^2}. \end{aligned} \quad (57)$$

Since $\mathbf{h}^H(\omega)\mathbf{h}(\omega)$ is a decreasing function of M ($M \geq 2$), it can be easily deduced from (56) that the white noise gain of the first-order DMA is an increasing function of M ($M \geq 2$). To better illustrate this, we take the first-order supercardioid pattern as an example and plot the value of $\mathbf{h}^H(\omega)\mathbf{h}(\omega)$ as a function of M in Fig. 29.

Then, we consider the second-order DMA, i.e., $N = 2$. Using (41)–(43) and with the help of (50)–(52), we can derive

$$\begin{aligned} \left|H_1(\omega)\right|^2 = a_0^2 &- \frac{a_0 a_2}{(\omega\tau_0)^2} \times \frac{40\left(M^2 - M - 2\right)}{3M^4 - 6M^3 - M^2 + 4M - 4} \\ &+ \frac{a_2^2}{(\omega\tau_0)^4} \times \frac{400\left(M^2 - M - 2\right)^2}{(3M^4 - 6M^3 - M^2 + 4M - 4)^2} \\ &+ \frac{a_1^2}{(\omega\tau_0)^2} \times \frac{36\left(2M^3 - 3M^2 - 3M + 2\right)^2}{(3M^4 - 6M^3 - M^2 + 4M - 4)^2} \end{aligned} \quad (58)$$

and

$$\begin{aligned} \sum_{i=2}^{M} \left|H_i(\omega)\right|^2 &= \frac{a_1^2}{(\omega\tau_0)^2} \times \frac{24\left(6M^3 - 9M^2 + M + 1\right)}{(M-1)M(3M^4 - 6M^3 - M^2 + 4M - 4)} \\ &+ \frac{a_2^2}{(\omega\tau_0)^4} \times \frac{480(2M-1)}{(M-1)M(3M^4 - 6M^3 - M^2 + 4M - 4)}. \end{aligned} \quad (59)$$

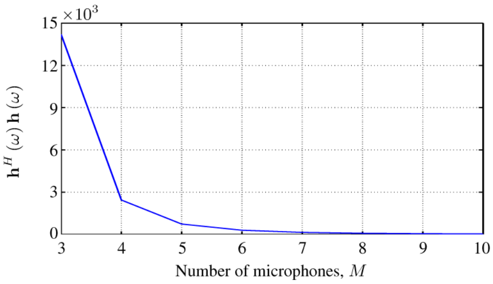

Fig. 30. The denominator of the white noise gain with the second-order DMA (supercardioid). $\delta = 0.5$ cm and $f = 1$ kHz.

As a result, the denominator of the white noise gain is

$$\begin{aligned}\mathbf{h}^H(\omega)\mathbf{h}(\omega) &= \sum_{m=1}^{M} |H_m(\omega)|^2 \\ &= a_0^2 - \frac{a_0 a_2}{(\omega\tau_0)^2} \times \frac{40\left(M^2 - M - 2\right)}{3M^4 - 6M^3 - M^2 + 4M - 4} \\ &\quad + \frac{a_2^2}{(\omega\tau_0)^4}\left[\frac{400\left(M^2 - M - 2\right)^2}{\left(3M^4 - 6M^3 - M^2 + 4M - 4\right)^2}\right. \\ &\quad \left. + \frac{480\left(2M - 1\right)}{\left(M - 1\right)M\left(3M^4 - 6M^3 - M^2 + 4M - 4\right)}\right] \\ &\quad + \frac{a_1^2}{(\omega\tau_0)^2}\left[\frac{36\left(2M^3 - 3M^2 - 3M + 2\right)^2}{\left(3M^4 - 6M^3 - M^2 + 4M - 4\right)^2}\right. \\ &\quad \left. + \frac{24\left(6M^3 - 9M^2 + M + 1\right)}{\left(M - 1\right)M\left(3M^4 - 6M^3 - M^2 + 4M - 4\right)}\right]. \qquad (60)\end{aligned}$$

The value of $\mathbf{h}^H(\omega)\mathbf{h}(\omega)$, as a function of M, is plotted in Fig. 30. It is seen that $\mathbf{h}^H(\omega)\mathbf{h}(\omega)$ is a decreasing function of $M (M \geq 3)$ and, therefore, it can be deduced from (56) that the white noise gain with the second-order DMA is an increasing function of $M (M \geq 3)$.

For $N > 2$, it can also be proved that the white noise gain with the Nth-order DMA is an increasing function of $M (M \geq N + 1)$, but we do not present the proof here since the equations are lengthy.

REFERENCES

[1] *Microphone arrays: Signal processing techniques and applications*, M. Brandstein and D. B. Ward, Eds.. Berlin, Germany: Springer-Verlag, 2001.

[2] Y. Huang, J. Benesty, and J. Chen*, Acoustic MIMO Signal Processing*. Berlin, Germany: Springer-Verlag, 2006.

[3] G. W. Elko and J. Meyer, "Microphone arrays," in *Springer Handbook of Speech Processing*, J. Benesty, M. M. Sondhi, and Y. Huang, Eds. Berlin, Germany: Springer-Verlag, 2008, ch. 50, pp. 1021–1041.

[4] J. Benesty, J. Chen, and Y. Huang*, Microphone Array Signal Processing*. Berlin, Germany: Springer-Verlag, 2008.

[5] J. Benesty, M. Souden, and Y. Huang, "A perspective on differential microphone arrays in the context of noise reduction," *IEEE Trans. Audio, Speech, Language Process.*, vol. 20, no. 2, pp. 699–704, Feb. 2012.

[6] J. Benesty and J. Chen*, Study and Design of Differential Microphone Arrays*. Berlin, Germany: Springer-Verlag, 2012.

[7] G. W. Elko, "Superdirectional microphone arrays," in *Acoustic Signal Processing for Telecommunication*, S. L. Gay and J. Benesty, Eds. Boston, MA, USA: Kluwer, 2000, ch. 10, pp. 181–237.

[8] H. F. Olson, "Gradient microphones," *J. Acoust. Soc. Amer.*, vol. 17, pp. 192–198, Jan. 1946.

[9] H. E. Ellithorn and A. M. Wiggins, "Antinoise characteristics of differential microphones," in *Proc. IRE*, Feb. 1946, pp. 84–89.

[10] H. Teutsch and G. W. Elko, "First- and second-order adaptive differential microphone arrays," in *Proc. IWAENC*, 2001.

[11] G. W. Elko, "Microphone array systems for hands-free telecommunication," *Speech Commun.*, vol. 20, pp. 229–240, Dec. 1996.

[12] M. Buck, "Aspects of first-order differential microphone arrays in the presence of sensor imperfections," *Eur. Trans. Telecomm.*, vol. 13, pp. 115–122, Mar.-Apr. 2002.

[13] M. Ihle, "Differential microphone arrays for spectral subtraction," in *Proc. IWAENC*, 2003.

[14] T. D. Abhayapala and A. Gupta, "Higher order differential-integral microphone arrays," *J. Acoust. Soc. Amer.*, vol. 127, pp. EL227–EL233, May 2010.

[15] E. De Sena, H. Hacihabiboğlu, and Z. Cvetković, "On the design and implementation of higher-order differential microphones," *IEEE Trans. Audio, Speech, Lang. Process.*, vol. 20, no. 1, pp. 162–174, Jan. 2012.

[16] A. I. Uzkov, "An approach to the problem of optimum directive antenna design," *Comptes Rendus (Doklady) de l'Academie des Sciences de l'URSS*, vol. LIII, no. 1, pp. 35–38, 1946.

Liheng Zhao received the B.E. degree in automation, and the Ph.D. degree in pattern recognition and intelligent system from University of Science and Technology of China, Hefei, China, in 2007 and 2012, respectively. He is currently a Postdoctoral Fellow at INRS-EMT, University of Quebec, in Montreal, Canada. His research interests include microphone array signal processing, audio signal processing, and speech technologies.

Jacob Benesty was born in 1963. He received a master degree in microwaves from Pierre & Marie Curie University, France, in 1987, and a Ph.D. degree in control and signal processing from Orsay University, France, in April 1991. During his Ph.D. (from Nov. 1989 to Apr. 1991), he worked on adaptive filters and fast algorithms at the Centre National d'Etudes des Telecomunications (CNET), Paris, France. From January 1994 to July 1995, he worked at Telecom Paris University on multichannel adaptive filters and acoustic echo cancellation. From October 1995 to May 2003, he was first a Consultant and then a Member of the Technical Staff at Bell Laboratories, Murray Hill, NJ, USA. In May 2003, he joined the University of Quebec, INRS-EMT, in Montreal, Quebec, Canada, as a Professor. He is also an Adjunct Professor at Aalborg University, in Denmark and at Northwestern Polytechnical University, Xi'an, Shaanxi, in China.

His research interests are in signal processing, acoustic signal processing, and multimedia communications. He is the inventor of many important technologies. In particular, he was the lead researcher at Bell Labs who conceived and designed the world-first real-time hands-free full-duplex stereophonic teleconferencing system. Also, he conceived and designed the world-first PC-based multi-party hands-free full-duplex stereo conferencing system over IP networks.

He was the co-chair of the 1999 International Workshop on Acoustic Echo and Noise Control and the general co-chair of the 2009 IEEE Workshop on Applications of Signal Processing to Audio and Acoustics. He is the recipient, with Morgan and Sondhi, of the IEEE Signal Processing Society 2001 Best Paper Award. He is the recipient, with Chen, Huang, and Doclo, of the IEEE Signal Processing Society 2008 Best Paper Award. He is also the co-author of a paper for which Huang received the IEEE Signal Processing Society 2002 Young Author Best Paper Award. In 2010, he received the "Gheorghe Cartianu Award" from the Romanian Academy. In 2011, he received the Best Paper Award from the IEEE WASPAA for a paper that he co-authored with Chen.

Jingdong Chen (M'99–SM'09) received the Ph.D. degree in pattern recognition and intelligence control from the Chinese Academy of Sciences in 1998.

From 1998 to 1999, he was with ATR Interpreting Telecommunications Research Laboratories, Kyoto, Japan, where he conducted research on speech synthesis, speech analysis, as well as objective measurements for evaluating speech synthesis. He then joined the Griffith University, Brisbane, Australia, where he engaged in research on robust speech recognition and signal processing. From 2000 to 2001, he worked at ATR Spoken Language Translation Research Laboratories on robust speech recognition and speech enhancement. From 2001 to 2009, he was a Member of Technical Staff at Bell Laboratories, Murray Hill, New Jersey, working on acoustic signal processing for telecommunications. He subsequently joined WeVoice Inc. in New Jersey, serving as the Chief Scientist. He is currently a professor at the Northwestern Polytechnical University in Xi'an, China. His research interests include acoustic signal processing, adaptive signal processing, speech enhancement, adaptive noise/echo control, microphone array signal processing, signal separation, and speech communication. Dr. Chen is currently an Associate Editor of the IEEE TRANSACTIONS ON AUDIO, SPEECH, AND LANGUAGE PROCESSING, a member of the IEEE Audio and Electroacoustics Technical Committee, and a member of the editorial advisory board of the *Open Signal Processing Journal*. He was the Technical Program Co-Chair of the 2009 IEEE Workshop on Applications of Signal Processing to Audio and Acoustics (WASPAA) and the Technical Program Chair of IEEE TENCON 2013, and helped organize many other conferences. He co-authored the books *Study and Design of Differential Microphone Arrays* (Springer-Verlag, 2013), *Speech Enhancement in the STFT Domain* (Springer-Verlag, 2011), *Optimal Time-Domain Noise Reduction Filters: A Theoretical Study* (Springer-Verlag, 2011), *Speech Enhancement in the Karhunen-Loève Expansion Domain* (Morgan&Claypool, 2011), *Noise Reduction in Speech Processing* (Springer-Verlag, 2009), *Microphone Array Signal Processing* (Springer-Verlag, 2008), and *Acoustic MIMO Signal Processing* (Springer-Verlag, 2006). He is also a co-editor/co-author of the book *Speech Enhancement* (Berlin, Germany: Springer-Verlag, 2005).

Dr. Chen received the 2008 Best Paper Award from the IEEE Signal Processing Society (with Benesty, Huang, and Doclo), the best paper award from the IEEE Workshop on Applications of Signal Processing to Audio and Acoustics (WASPAA) in 2011 (with Benesty), the Bell Labs Role Model Teamwork Award twice, respectively, in 2009 and 2007, the NASA Tech Brief Award twice, respectively, in 2010 and 2009, the Japan Trust International Research Grant from the Japan Key Technology Center in 1998, and the Young Author Best Paper Award from the 5th National Conference on Man-Machine Speech Communications in 1998.